Journal of Magnetism and Magnetic Materials 361 (2014) 57–60

Contents lists available at ScienceDirect

Journal of Magnetism and Magnetic Materials

journal homepage: www.elsevier.com/locate/jmmm

Microstructure effect on magnetization and domain structure in $Ni_{0.49}Zn_{0.49}Co_{0.02}Fe_{1.90}O_x$ ferrite

K. Kawano [a,*], M. Kotsugi [b], T. Ohkochi [b]

[a] Taiyo Yuden Co., Ltd. Materials Research & Development Department, General R&D Laboratories, Japan
[b] Japan Synchrotron Radiation Research Institute / SPring-8, Japan

ARTICLE INFO

Article history:
Received 1 February 2013
Received in revised form
3 December 2013
Available online 24 February 2014

Keywords:
Ferrite
Magnetic domain
Grain size
PEEM

ABSTRACT

The effect that grain size has on magnetization in cobalt substituted NiZn polycrystalline bulk ferrite has been studied and the magnetic domain has been visualized by taking measurements with a Photoemission Electron Microscope (PEEM). Complex permeability shows that magnetization with a grain size smaller than ~6 μm is dominated only by the spin rotation and the magnetic domain wall motion contributes when the grain size is larger. PEEM measurements show that the small grain induces the small magnetic domain and it becomes larger when the grain is large, which is a result that agrees with the magnetization process. At the same time, the presence of a domain wall across the grain boundary has been confirmed regardless of the grain size. This suggests the possibility of there being a magnetic coupling between the grains related to the effect that the microstructure has on magnetic domain structure and magnetization in cobalt substituted NiZn ferrite.

1. Introduction

The effect that the microstructure of polycrystalline NiZn ferrite has on its magnetic domain structure is one of key factors in understanding its magnetic properties. It has been reported that a small grain restricts the establishment of an intra-granular magnetic domain wall inside the grain, and the magnetic properties are dominated by the spin rotation [1,2,3]. This interpretation indicates that the magnetic domain wall is located at the grain boundary and each grain behaves as a single magnetic domain when the grain size is sufficiently small. Furthermore, magnetization dominated by the spin rotation reduces the core loss with a small external magnetic field [4]. As described above, the microstructure clearly affects the magnetization of NiZn ferrite, but still several questions remain. For instance, cobalt substituted polycrystalline NiZn (hereafter NiZnCo) ferrite with an average grain size that is smaller than ~6 μm shows magnetization dominated by the spin rotation, without a contribution from the domain wall motion. Nevertheless, it is obvious that there are some grains with a size that is larger than average in these polycrystalline samples and some exceed ~10 μm. This gives rise to the question of whether or not such large grains in the sample with an average grain size smaller than ~6 μm have a single magnetic domain. Another possibility cannot be ruled out: different kinds of magnetic domains corresponding to the different local structures may coexist in polycrystalline NiZnCo ferrite. Therefore, it is important to understand the relationship between the magnetization process and the magnetic domain structure and how the microstructure affects them.

Valuable knowledge might be obtained from visualizing the magnetic domain; however, there are not many reports about visualizing the magnetic domain in NiZnCo ferrite for several reasons such as the very small Kerr effects and rough sample surface. Magnetic Force Microscope (MFM) has been used to visualize the magnetic domain of ferrite, and it has been reported that grains larger than ~4 μm have an intra-magnetic domain boundary inside them, and smaller grains do not [5]. In order to understand how the microstructure affects the magnetic domain structure and magnetization of polycrystalline NiZnCo ferrite, the magnetization process has been investigated using samples with different grain sizes. The Photoemission Electron Microscope (PEEM) technique has been used with synchrotron X-rays to visualize the magnetic domain structure of NiZnCo ferrite.

2. Experiments

The polycrystalline $Ni_{0.49}Zn_{0.49}Co_{0.02}Fe_{1.90}O_x$ ferrite materials used in this study were fabricated with the conventional ceramic sintering method [3]. Commercially available raw materials of Fe_2O_3, NiO, CoO and ZnO were mixed together. The mixed powders

* Corresponding author.

http://dx.doi.org/10.1016/j.jmmm.2014.02.048
0304-8853

Table 1
Sample details with sintering temperature, density and grain size determined from SEM images.

Sample	Sintering temp(°C)	Density(g/cm^3)	Grain size(μm)
1	1150	5.25	4.5
2	1200	5.21	6.4
3	1300	5.23	10.5

were calcined in air at 900 °C for 2 h, and the calcined powder was reground. The average particle size of the spinel ferrite after grounding was less than 1 μm. The powder was mixed with an appropriate amount of PVA binder, and uniaxially pressed under pressure to form not only a toroidal shape, so that the complex permeability and DC magnetization curve could be examined, but also a disc shape, so that PEEM measurements could be performed. These samples were pre-heated to remove the binder. The average grain size was controlled by adjusting the sintering temperature and determined by averaging more than 300 measurements performed by Scanning Electron Microscope (SEM). All samples were investigated by X-ray diffraction (XRD) using CuKα radiation to identify the phases. Details of all samples are listed in Table 1 along with the sintering temperature, density and grain size. Before performing PEEM measurements, the surface of the sample was carefully treated with an automatic mechanical polisher and finished by a buff polishing. After polishing, the samples were thermally etched at a temperature lower than the sintering temperature in order to remove the residual stress induced while polishing.

The complex permeability was measured using an Agilent 4991A impedance analyzer. A Riken-Denshi DC B-H CURVE TRACER was used to measure the DC magnetization curves.

PEEM experiments were performed at BL17SU beam line (a-branch) in SPring-8 [6,7]. The right and left circularly polarized X-rays generated from a multi-polarization-mode undulator were used in this study. We applied a spectroscopic photoemission/low-energy-electron microscope (SPELEEM, ELMITEC Co., Ltd.) with which we can obtain high resolution (better than 50 nm) PEEM images. Chemical maps (X-ray absorption spectroscopic (XAS)–PEEM images) and magnetic domain images (X-ray magnetic circular dichroism; (XMCD)–PEEM images) of samples of NiZnCo ferrite were obtained at Fe L_3-edge (708 eV). In order to achieve PEEM imaging on poorly conducting ($\sim 10^6\ \Omega$ cm) samples of NiZnCo ferrite without considerable charging, a thick Au film was deposited *ex situ* on the sample except for a narrow window area with a width of 30 μm. Local electronic conductivity at the observation area was ensured by continuously illuminating with X-rays for ~30 min and the surrounding Au films allowed the created positive charges to be released at ground level. Details of the measurement method used for insulator materials will be reported in another paper. [8]. All experiments were performed at room temperature and with zero external magnetic field.

3. Results and discussions

Fig. 1(a) shows the frequency dependence of the complex permeability of samples 1, 2 and 3. Similar results have been obtained from both samples 1 and 2 in spite of the different grain sizes, and sample 3 with the larger grain size than those of samples 1 and 2 has larger permeability. The frequency spectra can be expressed as a sum of the combination of the domain wall motion and spin rotation using the following equations: [9–11].

$$\mu(w) = 1 + \chi_{spin}(w) + \chi_{dw}(w) \quad (1)$$

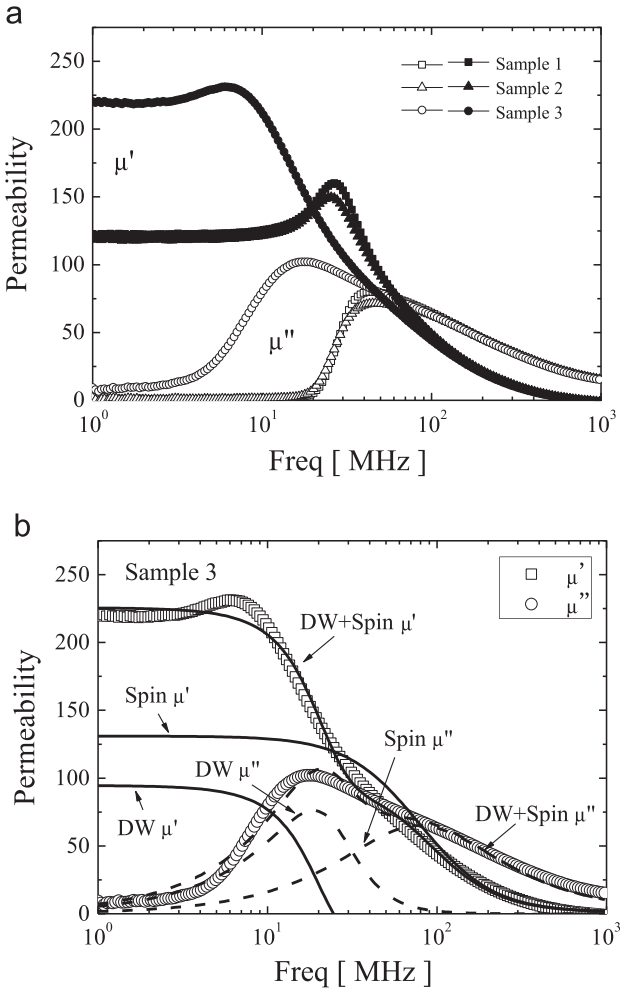

Fig. 1. (a) The complex permeability dispersion of samples 1, 2 and 3. The black and white dots are the real and imaginary parts of the permeability respectively. (b) The experimental result of sample 3 was analyzed with Eqs. (1)–(3). Data was fitted by the least squares method and the best fitting result was shown as the solid line in this figure with K_s=130, K_{dw}=95, w_{spin}=79 MHz, w_{dw}=24 MHz and β=34 MHz in these equations.

$$\chi_{spin}(w) = \frac{K_s}{1 + i(w/w_{spin})} \quad (2)$$

$$\chi_{dw}(w) = \frac{K_{dw} w_{dw}^2}{w_{dw}^2 - w^2 + i\beta w} \quad (3)$$

where $\chi_{spin}(w)$ and $\chi_{dw}(w)$ are the components of the spin rotation and domain wall motion. K_s and K_{dw} are the static susceptibilities of the spin and domain wall motion. w_{spin} and w_{dw} are the resonance frequencies of the spin and domain wall. β in Eq.(3) is the damping factor of the domain wall motion. The complex permeability of sample 3 was analyzed using these equations, and the results are shown in Fig. 1(b) as the solid (real) and dotted (imaginary) lines. The fitting results show a good agreement with the measured values, and the contribution from the spin rotation and domain wall motion could be deduced separately. An important aspect is that the contribution from the spin rotation in sample 3 is almost the same as the measured results of samples 1 and 2. This result strongly suggests that the permeability of samples 1 and 2 is dominated by the spin rotation without the contribution of the domain wall motion because the grains are too small to establish an intra-granular domain wall inside the grain. Such understanding indicates that the grains in samples 1 and